Cell, Vol. 94, 181–191, July 24, 1998, Copyright ©1998 by Cell Press

Crystal Structure of the Signal Sequence Binding Subunit of the Signal Recognition Particle

Robert J. Keenan,*‡ Douglas M. Freymann,*§ Peter Walter,*† and Robert M. Stroud*
*Department of Biochemistry and Biophysics
†The Howard Hughes Medical Institute
School of Medicine
University of California
San Francisco, California 94143-0448

Summary

The crystal structure of the signal sequence binding subunit of the signal recognition particle (SRP) from *Thermus aquaticus* reveals a deep groove bounded by a flexible loop and lined with side chains of conserved hydrophobic residues. The groove defines a flexible, hydrophobic environment that is likely to contribute to the structural plasticity necessary for SRP to bind signal sequences of different lengths and amino acid sequence. The structure also reveals a helix-turn-helix motif containing an arginine-rich α helix that is required for binding to SRP RNA and is implicated in forming the core of an extended RNA binding surface.

Introduction

The signal recognition particle (SRP) is a ribonucleoprotein complex that mediates the cotranslational targeting of nascent secretory and membrane proteins to the endoplasmic reticulum (Walter and Johnson, 1994; Rapoport et al., 1996). Signal sequences that emerge from the ribosome as part of the nascent chain are bound by the 54 kDa subunit of the SRP (SRP54), creating a cytosolic targeting complex that is directed to the endoplasmic reticulum membrane via an interaction with the SRP receptor (Gilmore et al., 1982a, 1982b; Meyer et al., 1982). GTP binding to SRP and to the SRP receptor stabilizes the SRP-SRP receptor complex (Bacher et al., 1996; Rapiejko and Gilmore, 1997) and leads to dissociation of SRP from the nascent chain and the ribosome (Connolly and Gilmore, 1989). Subsequently, translation resumes, and the nascent chain is directed into or across the membrane by the protein translocation machinery of the cell. Upon hydrolysis of GTP by the SRP-SRP receptor complex, SRP is released from the receptor to initiate a new round of targeting (Connolly et al., 1991).

The mechanism of cotranslational targeting to the endoplasmic reticulum membrane of eukaryotes and to the plasma membrane of prokaryotes is evolutionarily conserved. Components of the prokaryotic cotranslational targeting pathway, Ffh, 4.5S RNA, and FtsY, share sequence and functional conservation with their eukaryotic counterparts, SRP54, SRP RNA, and the SRP receptor. Ffh is essential for viability of *Escherichia coli* (Phillips and Silhavy, 1992), and inhibition of the SRP-dependent cotranslational targeting pathway blocks the insertion of a subset of *E. coli* inner membrane proteins (Ulbrandt et al., 1997). Ffh can be cross-linked to signal sequences in crude *E. coli* extracts (Luirink et al., 1992; Valent et al., 1995) and substitutes for the signal sequence binding activity of SRP54 when reconstituted into a chimeric particle in mammalian translation extracts (Bernstein et al., 1993). During targeting, the Ffh-4.5S RNA complex binds tightly to FtsY in a GTP-dependent manner, resulting in the reciprocal stimulation of GTP hydrolysis by Ffh and FtsY (Miller et al., 1994; Powers and Walter, 1995).

SRP54/Ffh is comprised of three domains, termed N, G, and M. The amino-terminal N domain is a four-helix bundle that is closely associated with the G domain, a Ras-like GTPase with an additional subdomain unique to the SRP family of GTPases (Freymann et al., 1997). Structurally related N and G domains are also present in the SRP receptor (Montoya et al., 1997). The N and G domains mediate the interaction of SRP with the SRP receptor (Zopf et al., 1993). The carboxyl-terminal M domain contains the SRP RNA-binding site and is required for binding to signal sequences (Römisch et al., 1990; Zopf et al., 1990; Lütcke et al., 1992).

A central unanswered question is how the hydrophobic signal sequence of the nascent chain is bound by SRP. Signal sequences that target proteins for secretion or membrane integration differ widely in length and in amino acid sequence and are remarkably tolerant of amino acid substitutions, so long as their hydrophobic character is retained (von Heijne, 1985; Valent et al., 1995; Zheng and Gierasch, 1996). Thus, SRP54/Ffh encodes specificity for a wide variety of signal sequences. Conceptually similar issues arise in other intracellular protein sorting events, such as protein sorting to mitochondria, in which sorting signals are specifically recognized by their cognate receptors yet share no defined sequence conservation.

To understand the structural basis of SRP54/Ffh function, we determined the crystal structure of Ffh from the thermophilic bacterium, *Thermus aquaticus*. The structure provides insight into the mechanism of signal sequence binding by SRP and into the nature of the interaction of SRP54/Ffh with SRP RNA.

Results

Structure Solution and Refinement

Recombinant *T. aquaticus* Ffh (residues 1–425) was purified from *E. coli* and crystallized in three different space groups in the presence of different detergents. These three crystal forms share a trimeric packing arrangement. The tetragonal crystal (space group $P4_12_12$, Table 1) was solved initially by isomorphous replacement using mercury and selenomethionine derivatives, phase

‡To whom correspondence should be addressed.
§Present address: Department of Molecular Pharmacology and Biological Chemistry, Northwestern University Medical School, Chicago, Illinois 60611.

Table 1. Summary of Crystallographic Statistics

Data Collection				
	Native	$HgCH_3$	SeMet	Native
Data set	Tetragonal[a]	Tetragonal	Tetragonal	Rhombohedral
Beamline	SSRL 7-1	CHESS A1	SSRL 7-1	CHESS F1
Detector	Mar30cm IP	Princeton 1K CCD	Mar30cm IP	Princeton 2K CCD
Wavelength (Å)	1.08	0.910	1.08	0.928
Space group	$P4_12_12$	$P4_12_12$	$P4_12_12$	R32
Resolution (Å)	3.2	3.8	3.4	3.2
Observations	216,587	89,883	83,109	105,880
Unique	27,678	14,259	19,813	34,343
Completeness (%)	99.6	82.9	83.5	84.5
R_{sym} (%)[b]	7.0	8.1	7.1	6.4
Average I/σI	17.7	13.9	12.6	10.8
MIR Analysis (Tetragonal)				
Data set		$HgCH_3$	SeMet	
Resolution cutoff (Å)		4.0	3.6	
No. of sites		3	27	
Phasing power (MLPHARE)[c]		0.72	1.02	
R_{cullis}[d]		0.84	0.74	
Overall figure of merit to 4.0 Å = 0.36				
Refinement Statistics (Rhombohedral)				
No. of reflections, F > σF (working/test)			30,645/1,569	
No. of non-hydrogen atoms			9,383	
Resolution (Å)			20.0–3.2	
R_{cryst}/R_{free} (%)[e]			24.5/27.1	
Average B factor (Å^2)			82.2	

[a] The tetragonal crystal form diffracts anisotropically beyond ~3.4 Å; reflections are observed to ~2.9 Å.
[b] $R_{sym} = \Sigma_i|I_i - \langle I_i\rangle|/\Sigma_i I_i$, where $\langle I_i\rangle$ is the average intensity over symmetry equivalents.
[c] Phasing power $= \langle F_h\rangle/\langle E\rangle$, where $\langle F_h\rangle$ is the rms of the heavy-atom structure factor amplitude and $\langle E\rangle$ is the rms lack of closure error.
[d] $R_{cullis} = \Sigma|F_{ph} \pm F_p| - |F_h(calc)|/\Sigma|F_{ph} \pm F_p|$ for centric reflections.
[e] $R_{cryst} = \Sigma|F_o - F_c|/\Sigma F_o$. R_{free} was calculated for a subset of reflections (~5%) omitted from the refinement.

combination using the previously determined structure of the N and G domains (Freymann et al., 1997), and 3-fold noncrystallographic symmetry averaging. Due to anisotropic diffraction from these crystals, only a partial model of the M domain was built into the resulting electron density. Subsequently, rhombohedral crystals (space group R32, Table 1) were obtained and solved by molecular replacement using the partial Ffh trimer from the tetragonal crystal as a search model.

Unambiguous density for the N and G domains and continuous density for the M domain were obtained in 3-fold averaged electron density maps calculated using data from the rhombohedral crystal form (Figure 1). The entire M domain structure was determined and then

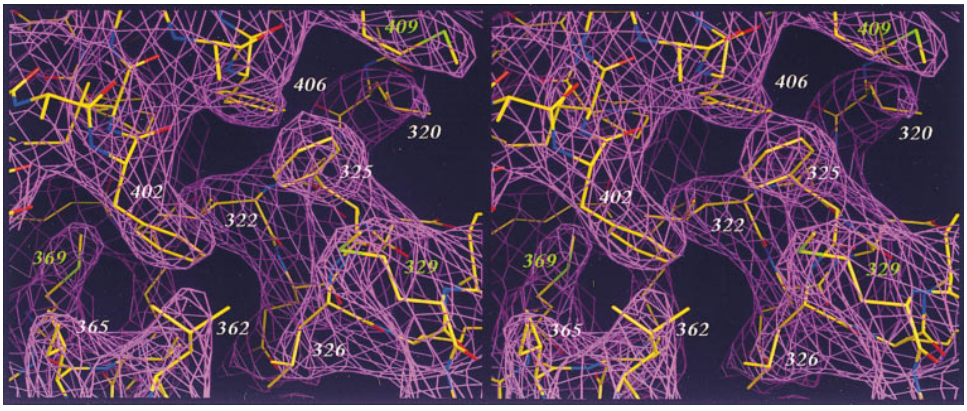

Figure 1. Stereo View of Electron Density in the M Domain

The electron density map, calculated at 3.2 Å resolution and contoured at 1σ, was obtained after 10 cycles of 3-fold NCS averaging in the rhombohedral dataset, starting with phases from the refined model of Ffh. The side chains of Leu-322, Ile-365, Met-369, and Phe-406 form part of the conserved hydrophobic core of the M domain. Leu-320, Phe-325, Leu-326, Met-329, Leu-362, Phe-402, and Met-409 contribute to the hydrophobic groove. Experimentally determined selenomethionine positions are observed for Met-329, Met-369, and Met-409 in the tetragonal crystal form.

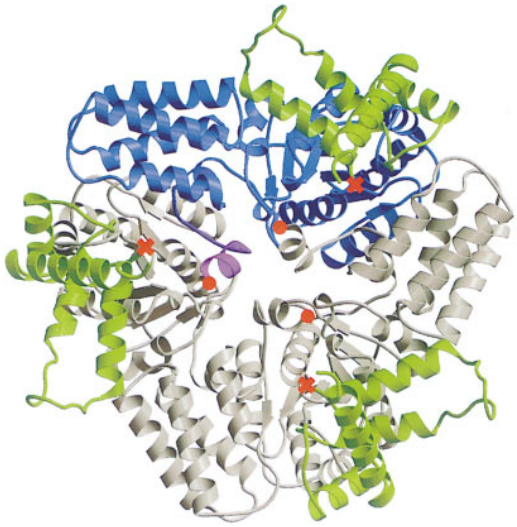

Figure 2. The Ffh Trimer Forming the Asymmetric Unit of the Rhombohedral and Tetragonal Crystal Forms

The N and G domains from one monomer are highlighted in blue, with its C-terminal helix, αH1, colored magenta. The N and G domains from the other two monomers are shown in gray, and the three M domains are shaded green. An 11-residue peptide that links the C terminus of the G domain (red circles) to the N terminus of the M domain (red crosses) is disordered; thus, the topological arrangement of M with respect to the N and G domains is ambiguous in the crystal.

The M domain forms loose contacts with the N domain from one molecule and the G domain from another, in the crystal. One of these contacts occurs close to the GTP-binding site of the G domain (possibly linking the signal sequence binding and GTPase functions of Ffh) and simultaneously places the M domain close to the conserved ALLEADV sequence of the N domain, which has been proposed to promote efficient signal sequence recognition (Newitt and Bernstein, 1997). A second contact occurs at the distal end of the N domain four-helix bundle. Given that the observed M domain contacts bury relatively little surface area and do not involve conserved amino acids, they may not represent functional interactions.

confirmed by the location of three experimentally observed selenium sites in the M domain of the tetragonal crystal form. The structure was refined with noncrystallographic symmetry restraints to a crystallographic R factor of 24.5% (R_{free} = 27.1%) at 3.2 Å resolution. All amino acids except for 11 in the linker region between the G and M domains and 7 amino acids at the extreme C terminus of the M domain are defined by the electron density; thus, the refined structure of Ffh includes residues 1–307 and 319–418.

Overall Structure of Ffh

The crystal structure of *T. aquaticus* Ffh reveals a three-domain protein. Extending from the C terminus of the G domain is a short helix (αH1), followed by an 11-amino-acid flexible linker that tethers the M domain to the N and G domains. Consistent with the observed proteolytic susceptibility of the linker peptide in solution (Römisch et al., 1990; Zopf et al., 1990), electron density for this region is weak, and we cannot determine which G domain is covalently attached to the M domain in the trimeric arrangement of the crystal (Figure 2). The structures of the N and G domains in the intact Ffh are essentially the same as in the previously determined

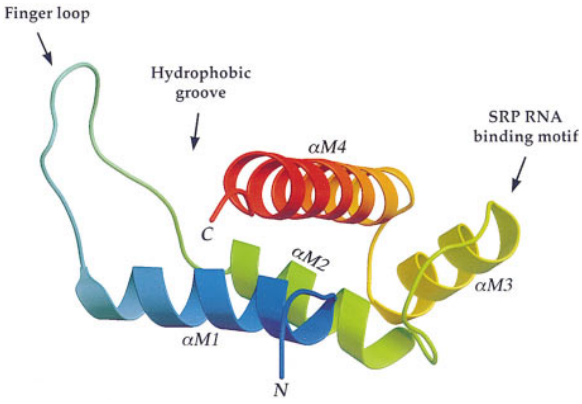

Figure 3. Structure of the M Domain

Ribbon representation of the M domain, colored blue to red from the N to the C terminus. Hydrophobic residues lining the proposed signal sequence binding groove are contributed from helix αM1, the flexible finger loop, helix αM2, and helix αM4. The highly conserved SRP RNA-binding motif is centered around helix αM3. Seven residues at the extreme C terminus of the M domain cannot be seen in the electron density map and are probably disordered.

structure of a proteolytically generated NG fragment (Freymann et al., 1997). However, there is an ~8° change in the disposition of the N domain relative to the G domain. A similar domain motion is observed between the GDP-bound form and the apo form of the NG fragment and may be functionally significant (D. M. F. et al., unpublished data).

Structure of the M Domain

The M domain consists of four amphipathic helices organized around a small hydrophobic core (Figure 3). Two antiparallel helices, αM1 and αM2, form the base of a deep groove that is bounded on one end by a 19-residue loop that connects αM1 to αM2 (the "finger loop") and on the other end, by helix αM4, which crosses αM1 and αM2 almost perpendicularly near the center of the domain. On the surface of the domain distal to the finger loop, helix αM3 is packed tightly against the conserved hydrophobic core of the M domain. The core is the most ordered region of the M domain and serves to organize two key functional surfaces of the domain, a hydrophobic groove that is implicated in signal sequence binding and an arginine-rich motif that is required for binding to SRP RNA.

The Hydrophobic Groove

The most prominent structural feature of the M domain is the deep groove formed by helices αM1, αM2, αM4, and the finger loop. The groove is approximately 25 Å long, 15 Å wide, and 12 Å deep and is comprised almost exclusively of hydrophobic amino acids (Figure 4, green and yellow). In total, 11 leucines, 3 phenylalanines, 3 methionines, 2 valines, and 2 isoleucines contribute to a hydrophobic surface area within the groove of more than 1487 $Å^2$. This comprises greater than 20% of the total surface area of the M domain. The size of the groove and the conserved hydrophobic character of the amino acid side chains that line it (Figure 5, shaded gray) suggest that the groove forms the signal sequence binding pocket of SRP.

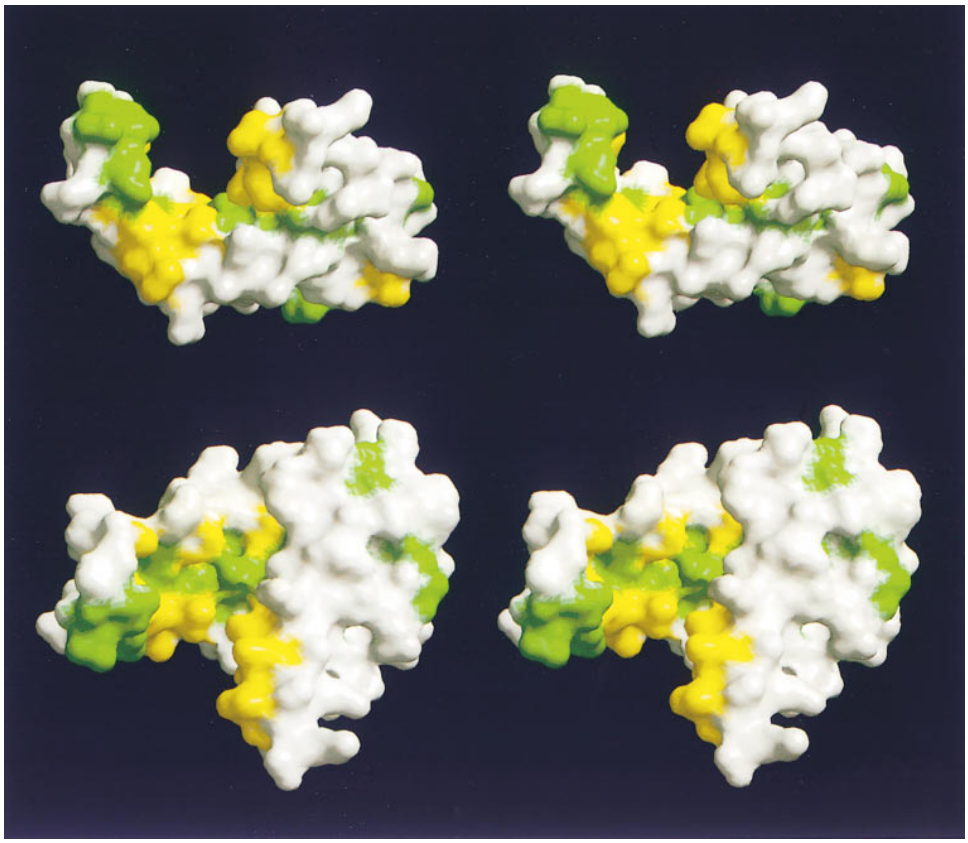

Figure 4. The Hydrophobic Groove of the M Domain

Stereo view of a molecular surface representation of the proposed signal sequence binding groove of Ffh. The top view corresponds closely to the orientation in Figure 3; the bottom view is rotated 90° about the horizontal axis with respect to the orientation in the top view. Hydrophobic residues (Met, Leu, Ile, Val, and Phe) in the *T. aquaticus* M domain are colored (green and yellow). A total of 14 positions that correspond to methionine in the sequence of *E. coli* Ffh are colored yellow. Of these, 11 are positioned to line the proposed signal sequence binding groove of Ffh. Six additional methionine residues are located at the extreme C terminus of *E. coli* Ffh and cannot be modeled in the *T. aquaticus* structure. Note the asymmetric distribution of hydrophobic residues in the groove.

In contrast to the relatively rigid helices αM1, αM2, and αM4 that flank the hydrophobic groove, the conserved, 19-amino-acid finger loop motif (residues 337–355) is flexible. The loop forms an extended structure that contributes conserved hydrophobic side chains to the interior surface of the groove. Gly-336–Pro-337 at the αM1-finger loop junction and Pro-346–Gly-347 at the tip of the loop are highly conserved (Figure 5) and flank a short stretch of residues that loosely adopt an α-helical conformation. The backbone flexibility of the finger loop is underlined by the fact that residues 352–354 in monomer C lie in a different conformation than those in monomers A or B in the trimeric arrangement of the crystal. The loop adopts yet a third conformation in a cubic crystal form. The implied flexibility of the finger loop is likely to be important for signal sequence binding (see Discussion).

In the crystal, pairs of M domains interlock such that the hydrophobic finger loop of one M domain (Figure 6, magenta) inserts into the hydrophobic groove of another (Figure 6, white). As a monomer in solution, this open conformation of the finger loop would expose the hydrophobic groove to solvent. Thus, the large hydrophobic surface area of the groove may explain why detergent is required to obtain well diffracting crystals of Ffh in the absence of signal sequences and for SRP to remain functional in vitro (Walter and Blobel, 1980).

The Arginine-Rich, Helix-Turn-Helix Motif

The M domain mediates the high affinity, high specificity interaction of SRP54/Ffh with SRP RNA. Deletion mutants constructed in *Bacillus subtilis* Ffh indicate that the equivalent region from αM2 to αM4 in *T. aquaticus* Ffh (residues Lys-353–Leu-416) is sufficient for specific binding of SRP RNA (Kurita et al., 1996). This region of the M domain contains a helix-turn-helix (HTH) motif that is structurally similar to those found in HTH DNA-binding proteins (Steitz et al., 1982). The α-carbon atoms of the 21 residues comprising the HTH motif in Ffh (from αM3 to αM4; residues 384–404) superimpose on the HTH motif of the *lac* repressor (Chuprina et al., 1993; Lewis et al., 1996) with an rms deviation of 0.55 Å (Figure 7A). Residues contributing to the compact hydrophobic core, including Ile-365 and Met-369 from helix αM2, Ile-388 from helix αM3, and Val-399 and Ile-403 from helix αM4, serve to orient the HTH motif and are conserved in the M domain sequence. Gly-393, located at the start of the turn between helices αM3 and αM4, is also conserved in the M domain sequence. A similar pattern of

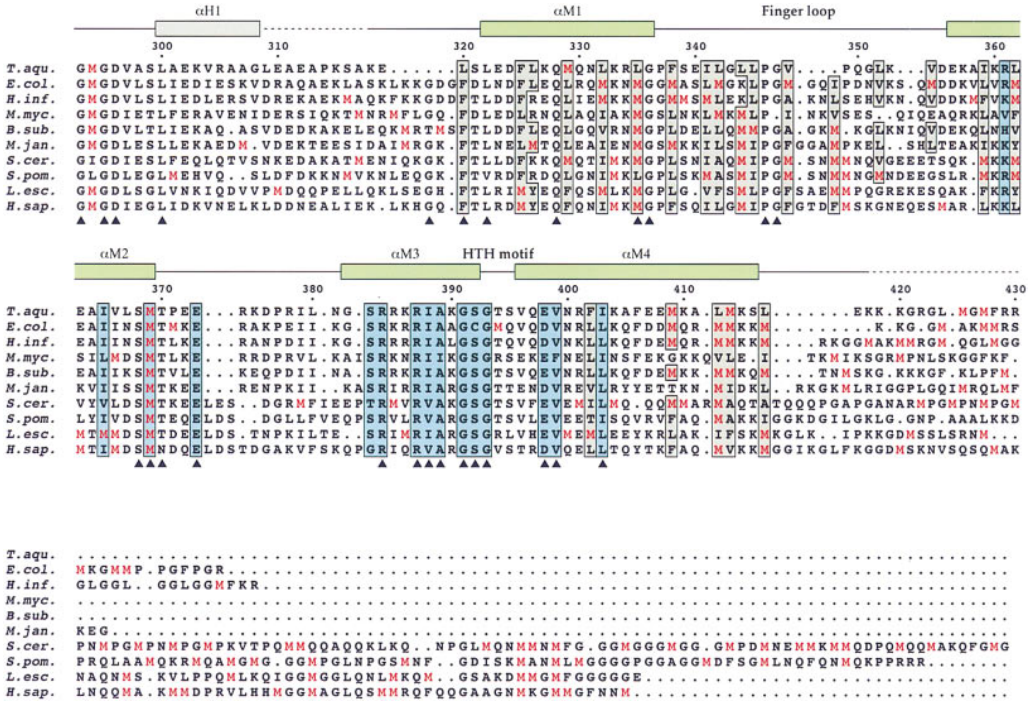

Figure 5. Sequence Alignment of the M Domain

Methionine residues are colored red. Conserved residues in the *T. aquaticus* Ffh crystal structure that line the hydrophobic groove are shaded gray; conserved residues in the SRP RNA-binding motif are shaded blue. The most conserved residues in the M domain are indicated with black triangles. Secondary structural elements and residue numbering based on the *T. aquaticus* sequence are shown above the aligned sequences. Sequences were obtained from the SWISS-PROT database and correspond to *T. aquaticus* (O07347), *E. coli* (P07019), *Haemophilus influenza* (P44518), *Mycoplasma mycoides* (Q01442), *B. subtilis* (P37195), *Methanococcus jannaschii* (Q57565), *Saccharomyces cerevisiae* (P20424), *Schizosaccharomyces pombe* (P21565), *Lycopersicon esculentum* (tomato, P49971), and *Homo sapiens* (P13624).

conserved hydrophobic and glycine residues is characteristic of the HTH sequence motif (Harrison and Aggarwal, 1990).

The M domain HTH motif contains a conserved, positively charged sequence, ^{384}RRKRIAKGSGTSVQEV^{399} (Althoff et al., 1994) (Figure 5, shaded blue). Mutational analysis indicates that Arg-384, Arg-387, and Lys-390 are essential for high affinity binding to SRP RNA (Kurita et al., 1996). These residues, along with basic residues at positions 385, 386, and 390, contribute to the positively charged RNA binding surface of the domain. Gly-391 and Gly-393 of the conserved GSG sequence are also essential for binding to SRP RNA (Kurita et al., 1996). In *E. coli* where Ser-392 is substituted by cysteine, binding of Ffh to SRP RNA protects this cysteine residue from chemical modification and, conversely, its alkylation impairs RNA binding (P. Peluso and P. W., unpublished results). These experimentally defined SRP RNA binding determinants are located on the side of the M domain opposite the hydrophobic groove and are centered on the first helix of the HTH motif, αM3 (residues 382–392; Figure 7B).

Discussion

Implications of the Structure for Signal Sequence–M Domain Interaction

The crystal structure of Ffh provides insight into the mechanism of signal sequence recognition by SRP. Cross-linking and functional studies have shown that the M domain of SRP54 contains the signal sequence binding site in SRP (Römisch et al., 1990; Zopf et al., 1990; Lütcke et al., 1992). The deep hydrophobic groove in the M domain is likely to provide this functionality. This assignment is consistent with mutational analyses in which deletion of a portion of *B. subtilis* Ffh, including αM1 and the majority of the finger loop, abolishes the ability of the protein to bind presecretory proteins (but not the ability to bind SRP RNA) in vitro (Takamatsu et al., 1997).

A striking feature of the M domain is its unusually high content of methionine residues, a feature that is phylogenetically conserved from bacterial to mammalian SRP (Bernstein et al., 1989) (Figure 5, red). The hydrophobic methionine side chain is flexible, both because it is unbranched and because of the unique conformational properties of the thioether linkage (Gellman, 1991). Combined with secondary structure predictions, these observations led to the proposal that methionine and other conserved hydrophobic residues in the M domain are arranged along amphipathic helices such that their flexible side chains form "bristles" lining a hydrophobic groove with sufficient plasticity to accommodate a variety of signal sequences (Bernstein et al., 1989). In *T. aquaticus*, however, many of the methionines whose abundance characterizes the M domains of mesophilic organisms are replaced by less flexible leucine, valine, and phenylalanine residues (Figure 5). This may

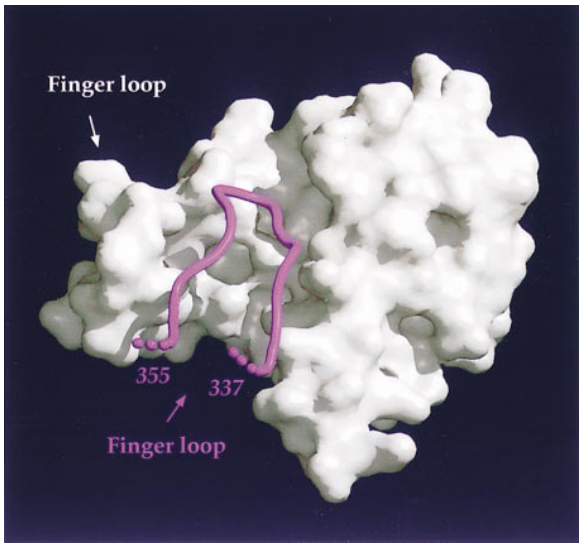

Figure 6. The Hydrophobic Groove of the M Domain Is Not Empty in the Crystal

The flexible finger loop of one M domain (magenta; residues 337–355 shown) inserts into the proposed signal sequence binding groove of another M domain (white, molecular surface representation), forming a hydrophobic cavity in the center of the groove that may contain detergent from the crystallization solution. This protein–protein interaction may represent an example of the extent to which the M domain has evolved to accommodate a wide variety of hydrophobic sequences.

represent an adaptation of the protein sequence to the organism's habitat at 75°C, a temperature at which thermal motion alone contributes substantially to side chain flexibility. Nevertheless, the positions of a total of 14 methionine residues located within the *E. coli* M domain can be inferred based on the *T. aquaticus* Ffh crystal structure and sequence alignment (Figure 5). Of these 14 residues, 11 line the hydrophobic groove (Figure 4, yellow), with the majority mapping onto the hydrophobic faces of α helices. Thus, a hydrophobic groove lined with the side chains of flexible amino acids is a conserved feature of the M domain and is likely to contribute to the ability of Ffh to bind different signal sequences.

The conformational variability observed in the finger loop of Ffh suggests that it has a role in the mechanism of binding and release of signal sequences. The finger loop may convert between open and closed conformations to compensate for the hydrophobic signal sequence when the binding site is unoccupied, possibly folding back into the groove that, in the Ffh crystal, is filled with the finger loop of an adjacent M domain. The backbone dynamics of the finger loop may also contribute to the plasticity necessary for SRP to bind different signal sequences.

The proposed signal sequence binding groove of Ffh is of sufficient size and hydrophobicity to accommodate signal sequences of different lengths and sequence. Signal sequences are typically between 20 and 30 residues in length and are characterized by a central hydrophobic core of approximately 10 to 15 residues flanked on either side by short stretches of polar residues (von Heijne and Abrahmsen, 1989). Isolated signal peptides are conformationally dynamic, with a tendency to adopt an α-helical conformation in nonpolar environments (Gierasch, 1989; McKnight et al., 1989). The dimensions of the hydrophobic groove are sufficient to accommodate $\sim$20 amino acids in an α-helical conformation or $\sim$16 amino acids in a fully extended β-hairpin conformation. In either conformation, binding to the M domain groove would expose one surface of the hydrophobic core of the signal sequence. The finger loop and a hydrophobic patch on the surface of the N or G domains are plausible candidates for a complementary hydrophobic region that could rearrange to cover this surface. The short stretches of polar residues that flank the core of signal sequences could be accommodated outside of the hydrophobic groove.

The C terminus of the M domain is variable in length, extending beyond helix αM4 for as few as $\sim$12 residues in *T. aquaticus* and for more than $\sim$100 residues in some eukaryotes (Figure 5, lower block of sequences). The significance of this region for signal sequence recognition is suggested by its proximity to the proposed signal sequence binding groove (Figure 3) and by the continued abundance of methionine residues (Figure 5). Deletion of 42 amino acids from the C terminus of mammalian SRP54 prevents cross-linking to signal sequences in vitro (Lütcke et al., 1992). By providing additional hydrophobic surface area adjacent to the groove, the C-terminal extensions present in higher organisms may increase the hydrophobic surface area available to facilitate binding of signal sequences or to increase the repertoire of sequences that can be recognized by SRP.

In the absence of SRP RNA, the *E. coli* M domain takes on properties of the molten globule state (Zheng and Gierasch, 1997). In the crystal structure, the M domain is less ordered than the N and G domains. The small hydrophobic core of the M domain is consistent with this mobility. A similar situation is encountered in the case of the 43-amino-acid HTH DNA-binding domain of $\gamma\delta$ resolvase, which is flexible in the absence of its DNA substrate (Yang and Steitz, 1995). The flexibility of the M domain may explain the notable difficulty in obtaining crystal or NMR structures of apo-SRP54/Ffh from mesophilic organisms.

Interesting parallels in macromolecular recognition may be drawn between binding of signal sequences by Ffh and the interaction of calmodulin (CaM) with its target proteins, both in terms of intrinsic flexibility and the structure of the interacting surfaces. CaM activates a variety of enzymes and proteins by binding to short sequences that, like the hydrophobic signal sequences recognized by SRP, share no obvious amino acid sequence homology. CaM has a dumbbell shaped structure in which two globular domains are connected by a flexible linker (Babu et al., 1988). Upon binding to protein substrates, this linker undergoes a conformational change that brings the globular domains of CaM together, engulfing the ligand in a hydrophobic tunnel (Ikura et al., 1992; Meador et al., 1992). Extensive hydrophobic contacts formed between CaM and its ligand are mediated by methionine side chains that are thought to confer plasticity to the binding site. In addition, flexibility of the linker peptide is thought to increase the promiscuity of CaM by allowing the two globular domains to adjust their orientation in response to different

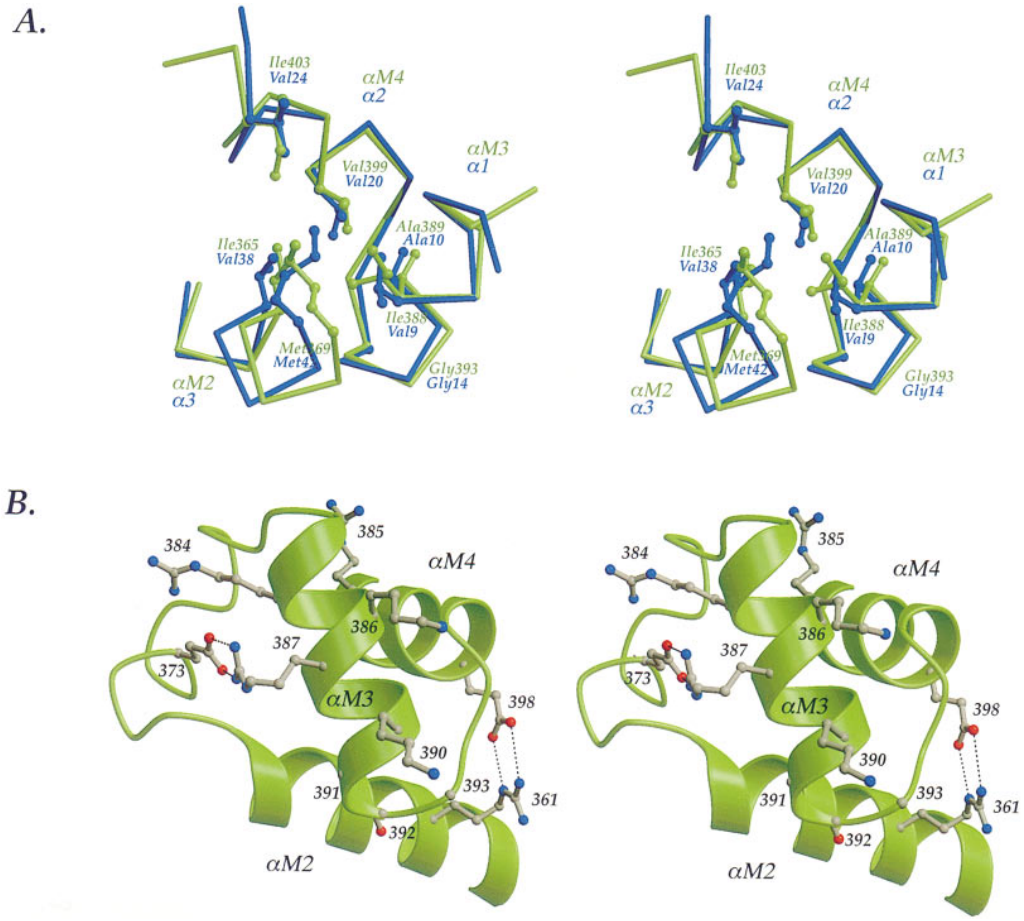

Figure 7. The Arginine-Rich, Helix-Turn-Helix Motif of the M Domain

(A) Stereo view of the HTH motif (αM3 to αM4) and a third helix (αM2) of the M domain (green) superimposed onto the corresponding region from the *lac* repressor (blue) (Chuprina et al., 1993). The least-squares overlap of α carbons was performed using LSQMAN (Kleywegt and Jones, 1994b). Conserved residues contributing to the compact hydrophobic core of the *lac* repressor are indicated, along with their counterparts in the M domain. Helix αM4 extends beyond helix α2 of the *lac* repressor by ~3 additional turns and contains basic residues at an extended C terminus; these characteristics are similar to the recognition helix of homeodomain DNA-binding proteins (Gehring et al., 1994).

(B) Stereo view of the conserved SRP RNA-binding motif of Ffh. This view is rotated ~90° about the vertical axis with respect to the orientation in Figure 7A. Positively charged side chains located in helix αM3 are likely to mediate the specific interaction of the M domain with SRP RNA. Arg-387 and Arg-361 form well-ordered salt bridges with the conserved residues Glu-373 and Glu-398, respectively.

ligands (Meador et al., 1993). In the case of SRP, the M domain by itself is sufficient for signal sequence binding; however, additional contacts with the N and G domains may also be involved (Zopf et al., 1993; Newitt and Bernstein, 1997; Zheng and Gierasch, 1997). Flexibility of the linker region may allow Ffh to adjust the orientation of the M domain relative to the N and G domains, so that peptides of different lengths and sequences can be accommodated.

Implications of the Structure for SRP RNA–M Domain Interaction

Sequence conservation (Althoff et al., 1994) combined with mutational and biochemical analysis (Kurita et al., 1996) of the M domain implicate residues within the first helix of the HTH motif, the arginine-rich helix αM3, in binding to SRP RNA. The location of these RNA binding determinants contrasts with the primary interaction of HTH DNA-binding proteins with their target DNAs, where binding is mediated by the second helix of the motif (the classical "recognition" helix) that inserts into the major groove of the DNA (Brennan, 1992). This suggests that Ffh and HTH DNA-binding proteins use distinct surfaces of the conserved HTH structural motif as the primary nucleic acid interaction site.

The Ffh-binding site on SRP RNA contains a conserved hairpin motif (termed domain IV) defined by three short double helices linked by one symmetric and one asymmetric internal loop (Poritz et al., 1988) (Figure 8A). Nucleotides in these loops are protected from chemical and enzymatic modification by contact with Ffh (Lentzen et al., 1996). Preliminary NMR assignments of domain IV of SRP RNA indicate that these conserved loops distort the A-form helix (Schmitz et al., 1996) (Behrens et al., unpublished results). In the case of another RNA-binding protein, HIV-1 Rev, binding to its cognate RNA is achieved by insertion of a basic α helix into a widened major groove (Battiste et al., 1996; Ye et al., 1996). The

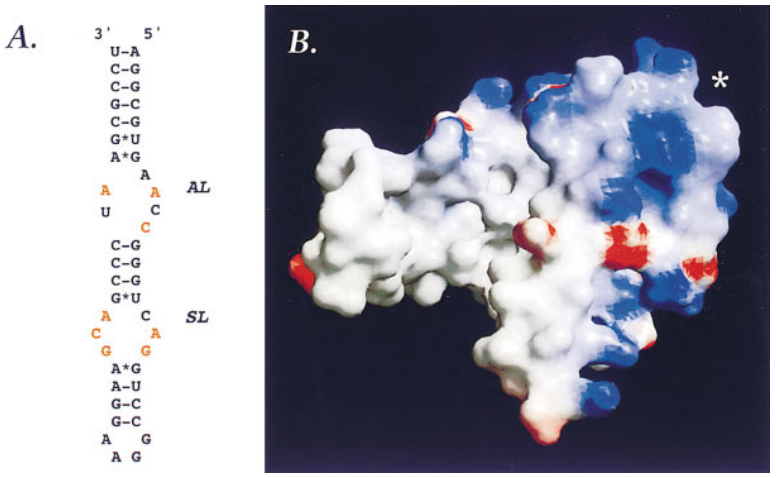

Figure 8. Implications for the M Domain–SRP RNA Interface

(A) The domain IV motif of SRP RNA from *Thermus thermophilus*. The conserved hairpin motif contains a symmetric (SL) and an asymmetric internal loop (AL) that are important for binding to SRP54/Ffh. Phylogenetically conserved nucleotides within the internal loops are highlighted in orange.

(B) Surface representation of the M domain colored according to local electrostatic surface potential (blue, positive; red, negative), calculated using GRASP (Nicholls, 1992). The positive charge character of the domain is centered around helix αM3 (indicated by an asterisk) and extends outward to include part of αM2, the αM2-αM3 loop, αM4, and the C terminus. In particular, the positive charges of Lys-357 and Arg-361 in αM2 are conserved, as is the overall basic charge distribution in the C terminus of the domain. SRP RNA may interact with a significant portion of the M domain.

primary interaction between the M domain and SRP RNA may also occur via insertion of helix αM3 into a distorted groove of SRP RNA.

The structural context of the SRP RNA-binding motif in the M domain may be critical to stabilize helix αM3 and to provide an additional RNA binding surface, since a peptide spanning the arginine-rich motif (corresponding to Arg-378–Arg-401 in *T. aquaticus*) derived from *B. subtilis* Ffh is, by itself, insufficient for RNA binding (Kurita et al., 1996). In this light, it is intriguing to note that the positively charged surface potential of the M domain extends outward from αM3 to include αM2, the αM2-αM3 loop region, αM4, and the C terminus (Figure 8B). Similarly, in HTH DNA-binding proteins the protein–nucleic acid binding surface is not restricted to the recognition helix (Rooman and Wintjens, 1996). Binding to SRP RNA stabilizes the M domain, suggesting formation of an extensive molecular interface (Zheng and Gierasch, 1997). Enzymatic and chemical modification (Lentzen et al., 1996) and preliminary NMR assignments (Behrens et al., unpublished results) indicate that the conserved asymmetric loop of domain IV induces a substantial bend in SRP RNA. Together, these observations suggest that SRP RNA attaches to the M domain by interaction with the conserved, arginine-rich helix αM3 and wraps around a significant portion of the M domain.

SRP responds to signal sequence binding and GTP occupancy by undergoing conformational changes that ultimately coordinate the steps required for accurate protein targeting to the translocation apparatus located in the membrane. SRP RNA plays a central role in this process, as underlined by its evolutionary conservation. Indeed, SRP RNA stimulates the interaction of Ffh with the SRP receptor, FtsY (Miller et al., 1994), and there is evidence suggesting that SRP RNA facilitates communication of the M domain with the N and G domains (Zheng and Gierasch, 1997). The structural juxtaposition of the proposed signal sequence and SRP RNA-binding sites in the M domain suggests that changes in signal sequence occupancy could lead to conformational changes in the M domain that are communicated to the SRP RNA, which in turn could affect interaction with the N and G domains and/or with other SRP ligands, including the ribosome and the SRP receptor.

Experimental Procedures

Protein Expression and Purification

A recombinant construct corresponding to residues 1–425 of Ffh from *T. aquaticus* was expressed in *E. coli* from a pET3c derivative in a BL21(DE3)/pLysE strain. Ten to fifteen milligrams of >98% pure protein were obtained from a liter of culture after purification using cation exchange chromatography and 70°C heat treatment. A series of cysteine mutants of Ffh were expressed and purified similarly. Selenomethionyl Ffh was prepared following the procedure of Van Duyne et al. (1993) and purified in the same manner as the wild-type protein.

Crystallization

Three different crystal forms of Ffh were obtained at room temperature using hanging drop vapor diffusion with a 20 mg/ml Ffh solution in 5 mM HEPES (pH 7.5). Tetragonal crystals were grown over reservoir solutions containing 1.2 M NaOAc, 0.1 M Tris (pH 8.5), 130 mM $CdSO_4$, and 2 mM cetyl trimethylammoniumbromide. They belong to space group $P4_12_12$ with a = 130.6 Å, c = 190.4 Å and contain ~55% solvent with three molecules in the asymmetric unit (as determined by Ficoll density gradient measurements). Cubic crystals were grown over reservoir solutions containing 1.2 M NaOAc, 0.1 M Tris (pH 8.5), 150 mM $CdSO_4$, and 2 mM Zwittergent 3-12. They belong to space group $P4_132$ with a = 155.6 Å and contain ~60% solvent with a single molecule of Ffh in the asymmetric unit. Rhombohedral crystals were grown over reservoir solutions containing 1.2 M NaOAc, 0.1 M Tris (pH 8.5), 120 mM $CdSO_4$, and 20 mM lithium dodecyl sulfate. They belong to space group R32, with a = 158.9 Å and α = 75.8°, and contain ~65% solvent, with three molecules in the asymmetric unit. The trimeric packing arrangement common to these three crystal forms of apo-Ffh does not reflect a physiologically important interaction, as there is no evidence for oligomerization of Ffh either in vitro or in vivo. Tetragonal crystals of an A203C mutant prederivatized with methyl-mercury nitrate and of selenomethionyl Ffh were obtained under conditions similar to those used for wild-type protein.

Data Collection and Processing

All three crystal forms of Ffh diffracted weakly using laboratory X-ray sources; thus, data were collected at synchrotron X-ray sources from single crystals flash-frozen in a nitrogen stream at −170°C (summarized in Table 1). The cryoprotectant solution contained 1.5

M NaOAc, 0.1 M Tris (pH 8.5), 200 mM $CdSO_4$, the appropriate detergent, and 20% ethylene glycol. A low-resolution (4.0 Å) native cubic dataset was collected using a 30 cm MAR image plate at a wavelength of 1.08 Å (SSRL, BL 7-1; data not shown). All data were integrated and scaled using DENZO and SCALEPACK (Otwinowski, 1993) using the default, -3σ cutoff.

Structure Determination

Heavy atom sites in the A203C-HgMe tetragonal crystal were located in isomorphous difference Patterson maps. Subsequently, heavy atom parameters were refined and SIR phases calculated in MLPHARE (Collaborative Computational Project, 1994). The sequence-specific mercury site served to orient the known structure of the NG fragment into 3-fold NCS-averaged SIR electron density maps. A solvent mask calculated in SOLOMON (Collaborative Computational Project, 1994) indicated an unaccounted region of density that was interpreted as belonging to the M domain. A generous molecular mask was created around the N and G domains and around the unaccounted-for density of the M domain using MAMA (Kleywegt and Jones, 1994a). NCS averaging in RAVE (Jones, 1992) with phase combination (from the N and G domains model) and extension from 5.0–3.2 Å resulted in a map that revealed good density for the N and G domains, but only allowed visualization of the gross secondary structural features in the M domain. Subsequently, data from selenomethionyl Ffh were obtained, and 27 of 33 expected selenium sites were located easily in a difference Fourier map. MIR phases calculated in MLPHARE (Collaborative Computational Project, 1994) were used in combination with partial model phases as a starting point for additional cycles of NCS averaging. At this stage, helices αM1, αM2, and αM4 were identified, and continuous density was observed for the stretch of residues between αM2 and αM4. The location of three experimentally determined selenomethionine peaks in M domain (Met-329, Met-369, and Met-409) allowed sequence to be definitively assigned to αM1 and αM2.

Subsequently, we obtained rhombohedral crystals that do not suffer from the aniostropic diffraction of the tetragonal crystals. This form was solved by molecular replacement in AMORE (Collaborative Computational Project, 1994) using the partial model of the NCS trimer from the tetragonal crystal as a search model (R = 43.7%, CC = 59.1% after rotation/translation searches). The resulting 3-fold NCS averaged maps were of good quality and confirmed the sequence assignments made in the tetragonal crystal form. In addition, αM3 was identified and sequence was assigned from the end of αM2 through the end of αM4. The maps indicated that the mask used in the averaging procedure was drawn incorrectly around the finger loop, located at an M domain–M domain crystal contact. After reconstructing a new mask around the M domain, averaged maps revealed continuous density for the 19-residue finger loop connecting αM1 and αM2. The final RSTATS (Collaborative Computational Project, 1994) R factor and correlation coefficient after 10 cycles of averaging were 23.4% and 93.0%, respectively.

Model Building and Refinement

The model was built in the rhombohedral crystal form using O (Jones et al., 1991) and refined using X-PLOR (Brünger, 1996). The free R factor was used to guide each stage of the refinement. Positional and torsional simulated annealing refinement protocols with tight NCS restraints on all atoms were used initially. Subsequently, individual B-factor refinement was performed, and a bulk solvent correction was applied using all data with $F > \sigma F$ between 20.0 and 3.2 Å resolution. During the final stages of rebuilding and refinement, NCS restraints were removed from residues 296–307 in the hinge region and residues 345–356 in the finger loop. Refinement resulted in a final crystallographic R factor of 24.5% and a free R factor of 27.1% for all data ($F > \sigma F$) between 20.0 and 3.2 Å. The refined average B factor is 82.2 $Å^2$, consistent with the observed limit of diffraction due to disorder in the crystal lattice. The final model is composed of residues 1–307 and 319–418; 89% of the amino acids are in the most favorable region of the Ramachandran plot, and none are in disallowed regions (Laskowski et al., 1993).

Illustrations

Figures were generated using BOBSCRIPT, Robert Esnouf's extended version of MOLSCRIPT (Kraulis, 1991), and GRASP (Nicholls, 1992) and rendered using RASTER3D (Merritt and Anderson, 1994).

Acknowledgments

We thank P. Foster, E. Rutenber, and the staff at the Stanford Synchrotron Radiation Laboratory and the Cornell High Energy Synchrotron Source for assistance with data collection; R. Morse, P. Focia, S. LaPorte, and M. Butte for computational assistance; A. Shiau, A. Derman, U. Schmitz, C. Reyes, P. Peluso, and T. Powers for discussions; A. Frankel and R. Kelly for comments on the manuscript; and members of the Stroud, Walter, and Agard laboratories for advice provided at all stages. We also thank Tom Steitz for pointing out the structural similarity of the M domain to the HTH family of DNA-binding proteins. This work was supported by National Institutes of Health (NIH) Institutional Training Grant CA-09270 to R. J. K., by fellowships from the Herb Boyer Fund and the Biotechnology Program of the University of California to D. M. F., by NIH grant GM-24485 to R. M. S., and by NIH grant GM-32384 to P. W; P. W. is an Investigator of the Howard Hughes Medical Institute.

Received May 1, 1998; revised June 17, 1998.

References

Althoff, S., Selinger, D., and Wise, J.A. (1994). Molecular evolution of SRP cycle components: functional implications. Nucleic Acids Res. *22*, 1933–1947.

Babu, Y.S., Bugg, C.E., and Cook, W.J. (1988). Structure of calmodulin refined at 2.2 Å resolution. J. Mol. Biol. *204*, 191–204.

Bacher, G., Lutcke, H., Jungnickel, B., Rapoport, T.A., and Dobberstein, B. (1996). Regulation by the ribosome of the GTPase of the signal-recognition particle during protein targeting. Nature *381*, 248–251.

Battiste, J.L., Mao, H., Rao, S., Tan, R., Muhandiram, D.R., Kay, L.E., Frankel, A.D., and Williamson, J.R. (1996). Alpha helix-RNA major groove recognition in an HIV-1 Rev peptide-RRE RNA complex. Science *273*, 1547–1551.

Bernstein, H.D., Poritz, M.A., Strub, K., Hoben, P.J., Brenner, S., and Walter, P. (1989). Model for signal sequence recognition from amino-acid sequence of 54K subunit of signal recognition particle. Nature *340*, 482–486.

Bernstein, H.D., Zopf, D., Freymann, D.M., and Walter, P. (1993). Functional substitution of the signal recognition particle 54-kDa subunit by its Escherichia coli homologue. Proc. Natl Acad. Sci. USA *90*, 5229–5233.

Brennan, R.G. (1992). DNA recognition by the helix-turn-helix motif. Curr. Opin. Struct. Biol. *2*, 100–108.

Brünger, A.T. (1996). X-PLOR Version 3.843 (New Haven, Connecticut: Yale University).

Chuprina, V.P., Rullmann, J.A., Lamerichs, R.M., van Boom, J.H., Boelens, R., and Kaptein, R. (1993). Structure of the complex of *lac* repressor headpiece and an 11 base-pair half-operator determined by nuclear magnetic resonance spectroscopy and restrained molecular dynamics. J. Mol. Biol. *234*, 446–462.

Collaborative Computational Project (1994). The CCP4 suite: programs for protein crystallography. Acta Crystallogr. D *50*, 760–763.

Connolly, T., and Gilmore, R. (1989). The signal recognition particle receptor mediates the GTP-dependent displacement of SRP from the signal sequence of the nascent polypeptide. Cell *57*, 599–610.

Connolly, T., Rapiejko, P.J., and Gilmore, R. (1991). Requirement of GTP hydrolysis for dissociation of the signal recognition particle from its receptor. Science *252*, 1171–1173.

Freymann, D.M., Keenan, R.J., Stroud, R.M., and Walter, P. (1997). Structure of the conserved GTPase domain of the signal recognition particle. Nature *385*, 361–364.

Gehring, W.J., Qian, Y.Q., Billeter, M., Furukubo-Tokunaga, K., Schier, A.F., Resendez-Perez, D., Affolter, M., Otting, G., and Wüthrich, K. (1994). Homeodomain-DNA recognition. Cell *78*, 211–223.

Gellman, S.H. (1991). On the role of methionine residues in the sequence-independent recognition of nonpolar protein surfaces. Biochemistry *30*, 6633–6636.

Gierasch, L.M. (1989). Signal sequences. Biochemistry *28*, 923–930.

Gilmore, R., Blobel, G., and Walter, P. (1982a). Protein translocation across the endoplasmic reticulum: I. detection in the microsomal membrane of a receptor for the signal recognition particle. J. Cell Biol. *95*, 463–469.

Gilmore, R., Walter, P., and Blobel, G. (1982b). Protein translocation across the endoplasmic reticulum: II. isolation and characterization of the signal recognition particle receptor. J. Cell Biol. *95*, 470–477.

Harrison, S.C., and Aggarwal, A.K. (1990). DNA recognition by proteins with the helix-turn-helix motif. Annu. Rev. Biochem. *59*, 933–969.

Ikura, M., Clore, G.M., Gronenborn, A.M., Zhu, G., Klee, C.B., and Bax, A. (1992). Solution structure of a calmodulin-target peptide complex by multidimensional NMR. Science *256*, 632–638.

Jones, T.A. (1992). A, yaap, asap, @#*? A set of averaging programs. In Molecular Replacement, E.J. Dodson, S. Gover, and W. Wolf, eds. (Warrington, England: SERC Daresbury Laboratory), pp. 91–105.

Jones, T.A., Zou, J.Y., Cowan, S.W., and Kjelgard, M.W. (1991). Improved methods for building protein models in electron density maps and the location of errors in these models. Acta Crystallogr. A *47*, 110–119.

Kleywegt, G.J., and Jones, T.A. (1994a). Halloween...masks and bones. In From First Map to Final Model, S. Bailey, R. Hubbard, and D. Waller, eds. (Warrington, England: SERC Daresbury Laboratory).

Kleywegt, G.J., and Jones, T.A. (1994b). A super position. CCP4 Newsletter *31*, 9–14.

Kraulis, P.J. (1991). MOLSCRIPT: a program to produce both detailed and schematic plots of protein structures. J. Appl. Cryst. *24*, 946–950.

Kurita, K., Honda, K., Suzuma, S., Takamatsu, H., Nakamura, K., and Yamane, K. (1996). Identification of a region of Bacillus subtilis Ffh, a homologue of mammalian SRP54 protein, that is essential for binding to small cytoplasmic RNA. J. Biol. Chem. *271*, 13140–13146.

Laskowski, R.A., MacArthur, M.W., Moss, D.S., and Thornton, J.M. (1993). PROCHECK: a program to check the stereochemical quality of protein structures. J. Appl. Cryst. *26*, 283–291.

Lentzen, G., Moine, H., Ehresmann, C., Ehresmann, B., and Wintermeyer, W. (1996). Structure of 4.5S RNA in the signal recognition particle as studied by enzymatic and chemical probing. RNA *2*, 244–253.

Lewis, M., Chang, G., Horton, N.C., Kercher, M.A., Pace, H.C., Schumacher, M.A., Brennan, R.G., and Lu, P. (1996). Crystal structure of the lactose operon repressor and its complexes with DNA and inducer. Science *271*, 1247–1254.

Luirink, J., High, S., Wood, H., Giner, A., Tollervey, D., and Dobberstein, B. (1992). Signal-sequence recognition by an Escherichia coli ribonucleoprotein complex. Nature *359*, 741–743.

Lütcke, H., High, S., Römisch, K., Ashford, A.J., and Dobberstein, B. (1992). The methionine-rich domain of the 54 kDa subunit of signal recognition particle is sufficient for the interaction with signal sequences. EMBO J. *11*, 1543–1551.

McKnight, C.J., Briggs, M.S., and Gierasch, L.M. (1989). Functional and nonfunctional LamB signal sequences can be distinguished by their biophysical properties. J. Biol. Chem. *264*, 17293–17297.

Meador, W.E., Means, A.R., and Quiocho, F.A. (1992). Target enzyme recognition by calmodulin: 2.4 Å structure of a calmodulin-peptide complex. Science *257*, 1251–1255.

Meador, W.E., Means, A.R., and Quiocho, F.A. (1993). Modulation of calmodulin plasticity in molecular recognition on the basis of x-ray structures. Science *262*, 1718–1721.

Merritt, E.A., and Anderson, W.F. (1994). Raster3D Version 2.0: a program for photorealistic molecular structures. Acta Crystallogr. D *50*, 219–220.

Meyer, D.I., Krause, E., and Dobberstein, B. (1982). Secretory protein translocation across membranes-the role of the "docking protein". Nature *297*, 647–650.

Miller, J.D., Bernstein, H.D., and Walter, P. (1994). Interaction of E. coli Ffh/4.5S ribonucleoprotein and FtsY mimics that of mammalian signal recognition particle and its receptor. Nature *367*, 657–659.

Montoya, G., Svensson, C., Luirink, J., and Sinning, I. (1997). Crystal structure of the NG domain from the signal-recognition particle receptor FtsY. Nature *385*, 365–368.

Newitt, J.A., and Bernstein, H.D. (1997). The N-domain of the signal recognition particle 54-kDa subunit promotes efficient signal sequence binding. Eur. J. Biochem. *245*, 720–729.

Nicholls, A. (1992). GRASP Manual (New York: Columbia University).

Otwinowski, Z. (1993). Oscillation data reduction program. In Data Collection and Processing, L. Sawyer, N.W. Isaacs, S. Bailey, eds. (Warrington, England: SERC Daresbury Laboratory).

Phillips, G.J., and Silhavy, T.J. (1992). The E. coli ffh gene is necessary for viability and efficient protein export. Nature *359*, 744–746.

Poritz, M.A., Strub, K., and Walter, P. (1988). Human SRP RNA and E. coli 4.5S RNA contain a highly homologous structural domain. Cell *55*, 4–6.

Powers, T., and Walter, P. (1995). Reciprocal stimulation of GTP hydrolysis by two directly interacting GTPases. Science *269*, 1422–1424.

Rapiejko, P.J., and Gilmore, R. (1997). Empty site forms of the SRP54 and SR alpha GTPases mediate targeting of ribosome-nascent chain complexes to the endoplasmic reticulum. Cell *89*, 703–713.

Rapoport, T.A., Jungnickel, B., and Kutay, U. (1996). Protein transport across the eukaryotic endoplasmic reticulum and bacterial inner membranes. Annu. Rev. Biochem. *65*, 271–303.

Römisch, K., Webb, J., Lingelbach, K., Gausepohl, H., and Dobberstein, B. (1990). The 54-kDa protein of signal recognition particle contains a methionine-rich RNA binding domain. J. Cell Biol. *111*, 1793–1802.

Rooman, M., and Wintjens, R. (1996). Structural classification of HTH DNA-binding domains and protein-DNA interaction modes. J. Mol. Biol. *262*, 294–313.

Schmitz, U., Freymann, D.M., James, T.L., Keenan, R.J., Vinayak, R., and Walter, P. (1996). NMR studies of the most conserved RNA domain of the mammalian signal recognition particle (SRP). RNA *2*, 1213–1227.

Steitz, T.A., Ohlendorf, D.H., McKay, D.B., Anderson, W.F., and Matthews, B.W. (1982). Structural similarity in the DNA-binding domains of catabolite gene activator and cro repressor proteins. Proc. Natl. Acad. Sci. USA *79*, 3097–3100.

Takamatsu, H., Bunai, K., Horinaka, T., Oguro, A., Nakamura, K., Watabe, K., and Yamane, K. (1997). Identification of a region required for binding to presecretory protein in Bacillus subtilis Ffh, a homologue of the 54-kDa subunit of mammalian signal recognition particle. Eur. J. Biochem. *248*, 575–582.

Ulbrandt, N.D., Newitt, J.A., and Bernstein, H.D. (1997). The E. coli signal recognition particle is required for the insertion of a subset of inner membrane proteins. Cell *88*, 187–196.

Valent, Q.A., Kendall, D.A., High, S., Kusters, R., Oudega, B., and Luirink, J. (1995). Early events in preprotein recognition in E. coli: interaction of SRP and trigger factor with nascent polypeptides. EMBO J. *14*, 5494–5505.

Van Duyne, G.D., Standaert, R.F., Karplus, P.A., Schreiber, S.L., and Clardy, J. (1993). Atomic structures of the human immunophilin FKBP-12 complexes with FK506 and rapamycin. J. Mol. Biol. *229*, 105–124.

von Heijne, G. (1985). Signal sequences: the limits of variation. J. Mol. Biol. *184*, 99–105.

von Heijne, G., and Abrahmsen, L. (1989). Species-specific variation in signal peptide design: implications for protein secretion in foreign hosts. FEBS Lett. *244*, 439–446.

Walter, P., and Blobel, G. (1980). Purification of a membrane-associated protein complex required for protein translocation across the endoplasmic reticulum. Proc. Natl. Acad. Sci. USA *77*, 7112–7116.

Walter, P., and Johnson, A.E. (1994). Signal sequence recognition and protein targeting to the endoplasmic reticulum membrane. Annu. Rev. Cell Biol. *10*, 87–119.

Yang, W., and Steitz, T.A. (1995). Crystal structure of the site-specific recombinase $\gamma\delta$ resolvase complexed with a 34 bp cleavage site. Cell *82*, 193–207.

Ye, X., Gorin, A., Ellington, A.D., and Patel, D.J. (1996). Deep penetration of an alpha-helix into a widened RNA major groove in the HIV-1 rev peptide-RNA aptamer complex. Nature Struct. Biol. *3*, 1026–1033.

Zheng, N., and Gierasch, L.M. (1996). Signal sequences: the same yet different. Cell *86*, 849–852.

Zheng, N., and Gierasch, L.M. (1997). Domain interactions in E. coli SRP: stabilization of M domain by RNA is required for effective signal sequence modulation of NG domain. Mol. Cell *1*, 1–20.

Zopf, D., Bernstein, H.D., Johnson, A.E., and Walter, P. (1990). The methionine-rich domain of the 54 kd protein subunit of the signal recognition particle contains an RNA binding site and can be cross-linked to a signal sequence. EMBO J. *9*, 4511–4517.

Zopf, D., Bernstein, H.D., and Walter, P. (1993). GTPase domain of the 54-kDa subunit of the mammalian signal recognition particle is required for protein translocation but not for signal sequence binding. J. Cell Biol. *120*, 1113–1121.

Brookhaven Protein Data Bank Accession Number

Coordinates have been deposited with the accession number 2ffh.